

PHASE TRANSITIONS IN STRONGLY INTERACTING MATTER*

*H. Satz***

Bielefeld University, Bielefeld, Germany

We discuss the phase structure of hadronic matter in terms of the basic dynamical and geometrical features of hadrons. Increasing the density of constituents of finite spatial extension, by increasing the temperature T or the baryochemical potential μ , eventually “fills the box” and eliminates the physical vacuum. The corresponding transition as function of T and μ can be determined through percolation theory. At low baryon density, this means a fusion of overlapping mesonic bags to one large bag, while at high baryon density, hard-core repulsion restricts the spatial mobility of baryons. As a consequence, there are two distinct limiting regimes for hadronic matter.

PACS: 12.38.Mh; 25.75.Nq

INTRODUCTION

In recent years, the general features of the phase diagram of strongly interacting matter have become increasingly well established [1]. Lattice QCD studies at finite temperature and now also for some range of finite baryon density [2–5], combined with chiral symmetry restoration arguments [6–12], lead for physical quark masses to the phase structure illustrated in Fig. 1 as function of temperature T and baryochemical potential μ . Following a region of nonsingular but rapid crossover of thermodynamic observables around a quasi-critical temperature of 170–190 MeV, increasing μ leads to a critical point, beyond which the system shows a first-order transition from confined to deconfined matter.

We want to show here how to deduce such behavior from the basic dynamical and geometrical features of hadronic matter [13]. Our question thus is the follow-

*I first met Ludwik Turko 34 years ago, at the 17th Karpacz Winter School, February 1980, *Developments in the Theory of Fundamental Interactions*; Director: L. Turko. At that Winterschool, I gave a talk *On Critical Phenomena in Strong Interaction Physics*. It is a great pleasure to be here in Wroclaw now to celebrate Ludwik’s 70th birthday and to bring up to date what I had talked about so many years ago. It is obviously a good sign for our field and for Ludwik’s vision in 1980 that the topic is, if anything, even of more interest today than it was then.

**E-mail: satz@physik.uni-bielefeld.de

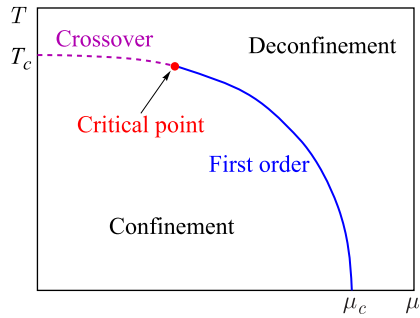


Fig. 1. Phase structure of QCD matter in the T - μ plane

size (with a radius $R_h \simeq 1$ fm) and can overlap or interpenetrate each other. For $\mu \simeq 0$, the contribution of baryons/antibaryons and baryonic resonances is relatively small, but with increasing baryon density, they form an ever larger section of the species present in the matter, and beyond some baryon density, they become the dominant constituents. Finally, at vanishing temperature, the medium consists essentially of nucleons.

At high baryon density, the dominant interaction is nonresonant. Nuclear forces are short-range and strongly attractive at distances of about 1 fm; but for distances around 0.5 fm, they become strongly repulsive. The former is what makes nuclei, the latter (together with Coulomb and Fermi repulsion) prevents them from collapsing. The repulsion between a proton and a neutron shows the purely baryonic “hard-core” effect and is connected neither to Coulomb repulsion nor to Pauli blocking of nucleons. As a consequence, the volumes of nuclei grow linearly with the sum of its protons and neutrons. With increasing baryon density, the mobility of baryons in the medium becomes strongly restricted by the presence of other baryons, leading to a “jammed” state, as shown in Fig. 2 [14].

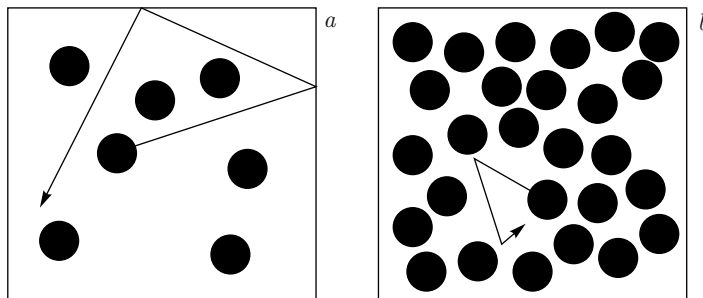


Fig. 2. Hard sphere states: full mobility (a), “jammed” (b)

ing: what conceptual aspects of hadronic interactions lead to the observed behavior, and, in particular, what features in hadronic dynamics result in the observed changes of the transition structure as function of T and μ ?

At low baryon density, the constituents of hadronic matter are mostly mesons, and the dominant interaction is resonance formation; with increasing temperature, different resonance species of increasing mass are formed, leading to a gas of ever increasing degrees of freedom. They are all of a typical hadronic

Increasing the density of constituents by increasing temperature, baryon density or both, leads to clustering of hadrons of spatial extension, and these clusters will eventually span the entire available volume. This onset of connectivity and the associated geometric critical behavior is the central topic of percolation theory, where the relevant thresholds have been determined for permeable spheres which can overlap (mesons), as well as for those which have an impenetrable hard core (baryons). In particular, one finds in both cases a geometric transition from a state in which the vacuum forms a finite part of the system to one in which only isolated bubbles of vacuum remain in a world of fully or partially overlapping hadrons. We shall consider this point of “disappearance” of a large-scale vacuum as the end of hadronic matter and calculate the corresponding limiting curve in the $T-\mu$ plane.

Our question therefore addresses two distinct situations. We have to consider the percolation of mesons, allowing full overlap, and then that of baryons with a hard core. In the next section, we shall first recall the salient features of percolation theory for the two cases. Following this, we will use a very simplistic toy model to illustrate the underlying concepts. In Sec. 3, we then turn to the realistic case of a hadronic resonance gas with baryon number and strangeness conservation. In the last section, we then consider the nature of the transition.

1. PERCOLATION

Here we briefly recall the essential results for the percolation of spheres, in three space dimensions, for the case of arbitrary overlap [15] and for spheres with an impenetrable hard core, allowing only partial overlap [16]. Consider N spheres of radius R_0 and hence volume $V_0 = (4\pi/3)R_0^3$ in a “box” of size V , with $V \gg V_0$. Percolation is said to occur when a connected and hence at least partially overlapping set of spheres spans the volume, or, in other words, when the volume occupied by the largest cluster of connected spheres reaches a finite fraction of V .

We address first the case of permeable spheres, i.e., with arbitrary overlap. In this case, when the density $n = N/V$ increases, clusters of overlapping spheres form, and for

$$n_m = \frac{\eta_m}{V_0}, \quad (1)$$

with $\eta_m \simeq 0.35$, the largest cluster first spans the system, i.e., percolation occurs [15]. At this point, the fraction

$$\phi_m = 1 - e^{-\eta_m} \simeq 0.30 \quad (2)$$

of space is occupied by spheres; the complementary 70% remain empty space (“vacuum”), which also still spans V . The largest cluster therefore has a density

of about $1.2/V_0$. In other words, at the percolation point, a randomly created state of a system of N spheres is very inhomogeneous, consisting mainly of one dense cluster and much empty space. A random distribution of extended constituents thus leads to something like a “geometric attraction” between point-like constituents with clustering as a result. We shall see later that in the percolation of hard-core spheres, this attraction is competing with an intrinsic repulsion.

For $n < n_m$, the clusters of overlapping spheres form only isolated bubbles in V . From Eq.(1) we see that at the percolation point, the total volume of all spheres adds up to 35% of the total volume; this is covered by the spheres to only 30%, indicating 5% “overlap”. After a further increase of density, a second percolation point is reached at

$$n_v = \frac{\eta_v}{V_0}, \tag{3}$$

where $\eta_v \simeq 1.22$. Now

$$\phi_v = 1 - e^{-\eta_v} \simeq 0.70 \tag{4}$$

is the fraction of space covered by spheres, with only 0.30 remaining empty. Here the sum of the sphere volumes is with 1.22 V considerably larger than the total volume, due to increased overlap. For $n \leq n_v$, the vacuum percolates, above n_v , only isolated bubbles of vacuum remain. In other words, for $n > n_v$, the vacuum has “disappeared” as a large-scale entity.

The existence of two percolation thresholds, one for the formation of the first spanning cluster of spheres and another for the disappearance of a spanning vacuum “cluster”, is a general feature of percolation theory in three or more dimensions.

We now turn to the percolation of spheres (again of radius R_0) having an impenetrable spherical hard core [16], which we assume to have the radius $R_c = R_0/2$. Each sphere now defines a volume $V_0 = (4\pi/3)R_0^3$, which is not accessible to the center of any other sphere. The spheres can partially overlap: the distance between their centers has to remain greater than $R_0 = 2R_c$. With increasing density, we now have again two percolation thresholds. At

$$n_m = \frac{\bar{\eta}_m}{V_0} \tag{5}$$

the spheres form a spanning cluster, and at

$$n_v = \frac{\bar{\eta}_v}{V_0} \tag{6}$$

the vacuum last spans the volume. Numerical studies [16] show that $\bar{\eta}_m \simeq 0.34$, practically the same as found above for permeable spheres of the same size. The percolation threshold for spheres with a hard core is on the dilute side, thus not much affected by the presence of the hard core, and we have a similar geometric

attraction. The vacuum percolation threshold, however, now is given by $\bar{\eta}_v \simeq 2.0$, in contrast to $\eta_v \simeq 1.24$ for permeable spheres. In other words, the disappearance of the vacuum requires for hard-core spheres a higher density than needed for permeable spheres. This is directly related to the hard-core repulsion, which tends to move the spheres apart and thus at high density counteracts tight clustering.

2. A TOY MODEL

In our simplified toy model, we want to compare the percolation behavior of an ideal gas of massless pions of radius R_h to that of an ideal gas of massive nucleons of the same size, but having a hard core of a (smaller) radius $R_c = R_h/2$. The density of pions is specified by the temperature T of the medium, that of the nucleons by the temperature T and the baryochemical potential μ , fixing the overall baryon number (nucleons minus antinucleons).

Consider first the system of pions. With three charge states, the density is given by

$$n_\pi(T) = 3 \frac{\pi^2}{90} T^3. \quad (7)$$

With increasing temperature, they will overlap and eventually fill the given volume with one big connected bag. When only isolated vacuum bubbles remain, we assume the system to have reached the limit of pionic matter. In the previous section it was shown that this occurs for

$$n_f = \frac{1.22}{V_h} \simeq 0.57 \text{ fm}^{-3}, \quad (8)$$

where $V_h = (4\pi/3)R_h^3$, and we have used $R_h = 0.8$ fm. Solving $n_h(T) = n_f$ yields

$$T_\pi \simeq \frac{0.96}{R_h} \simeq 240 \text{ MeV} \quad (9)$$

as the limiting temperature obtained through pion fusion. This value will drop slightly when we include nucleons and antinucleons, and it will decrease considerably when resonances are brought in, as we shall see in the next section.

The density of point-like nucleons of mass M is at $T = 0$ (when there are no antinucleons) determined in terms of the baryochemical potential μ ,

$$n_b(\mu, T = 0) = \frac{2}{3\pi^2} (\mu^2 - M^2)^{3/2}. \quad (10)$$

In the presence of a hard core of volume $V_c = V_h/8$, the density has to be calculated taking into account the reduction of the available volume. We approximate

this by a van der Waals approach [17], taking*

$$n_B(\mu, T = 0) = \frac{n_b(T, \mu)}{1 + n_b(T, \mu)V_e} \quad (11)$$

for the density of extended nucleons, where $V_e \simeq 2V_c$ denotes the excluded volume at random dense packing of hard spheres [19]. With increasing nucleon density, the box becomes more and more filled, and we saw above that the empty vacuum disappears for

$$\bar{n}_v \simeq \frac{2}{V_h} \simeq 0.93 \text{ fm}^{-3}, \quad (12)$$

taking the same radius for nucleons as for pions; this corresponds to about 5.5 times standard nuclear density $\rho_0 \simeq 0.17 \text{ fm}^{-3}$. Solving $n_B(T = 0, \mu) = \bar{n}_v$ yields

$$\mu_v \simeq 1.12 \text{ GeV} \quad (13)$$

for the limiting baryochemical potential at $T = 0$.

In the region of low to intermediate μ in the T - μ diagram, we approximate the density of point-like nucleons by the Boltzmann limit

$$n_b(\mu, T) \simeq \frac{2T^3}{\pi^2} \left(\frac{M}{T}\right)^2 K_2\left(\frac{M}{T}\right) e^{\mu/T} \simeq \frac{T^3}{2} \left(\frac{2M}{\pi T}\right)^{3/2} e^{(\mu-M)/T}, \quad (14)$$

where we have also used the large M/T form of the Bessel function $K_2(M/T)$. At $\mu = 0$, we can use this to add nucleons and antinucleons to the pions considered so far for filling the box. From

$$n_\pi + 2n_B = \frac{1.22}{V_h} \quad (15)$$

we then find a limiting temperature of hadronic matter

$$T_h \simeq 230 \text{ MeV} \quad (16)$$

slightly lower than for pions alone. The small change is due to the fact that nucleons amount to only about 6% of all hadrons at $\mu = 0$. If we there wanted to fill the box with only nucleons and antinucleons, we would have to go to the much higher temperature of about 430 MeV.

Using the approximation (14), we can ask for the value of μ at which the nucleon percolation curve crosses the hadronic limit T_h . Solving $n_B(T = T_h, \mu) = 2/V_h$ for μ , we find $\mu \simeq 0.8 \text{ GeV}$ for the crossing point. The comparative

*A thermodynamically consistent implementation of hard-core repulsion requires in addition a shift of μ [18], which for simplicity is neglected here.

behavior of the two curves is illustrated in Fig. 3. It is evident that at low nucleon density, pion percolation limits the hadronic matter density, while at high nucleon density, the percolation of hard spheres and the resulting jamming provide the limit. It should be emphasized, however, that the separate calculation of a (permeable) pion and a (hard-core) nucleon curve is obviously not the final solution, since a dilute admixture of nucleons and antinucleons contributes in the low density regime, just pions will help to reach percolation in the nucleonic region. We have followed an additive picture here, since so far (to our knowledge), continuum percolation studies have been performed either for permeable spheres or for spheres with a hard core. Evidently, what is needed here is a study allowing both types of constituents in a degree of mixture specified by μ , and this will lead to modifications in the intermediate region, as schematically included in Fig. 3.

We note here briefly that we can determine a confinement–deconfinement limit also by comparing the hadronic pressure to that of a quark–gluon plasma [17, 20]. Such a comparison leads by construction to a first-order transition in the entire T – μ plane. For $\mu = 0$, we then have

$$P_\pi = 3 \frac{\pi^2}{90} T^4 \quad (17)$$

for the pressure of an ideal massless pion gas, to be compared to

$$P_q = 37 \frac{\pi^2}{90} T^4 - B \quad (18)$$

for that of an ideal massless plasma of two quark flavours; here B denotes the bag pressure specifying the difference between coloured and physical vacua. Equating the two pressures (see Fig. 4, *a*) gives

$$T_c(B) = \left(\frac{90}{34\pi^2} \right)^{1/4} B^{1/4}, \quad (19)$$

so that by suitably tuning the bag pressure, we can obtain reasonable values for the transition temperature T_c .

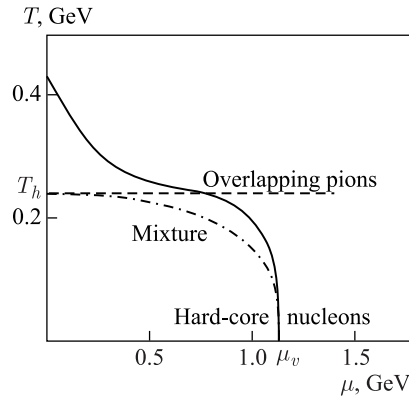


Fig. 3. Limit from massless pion percolation and from that of massive hard-core nucleons; the curve labelled “mixture” indicates the result expected of a combined percolation study

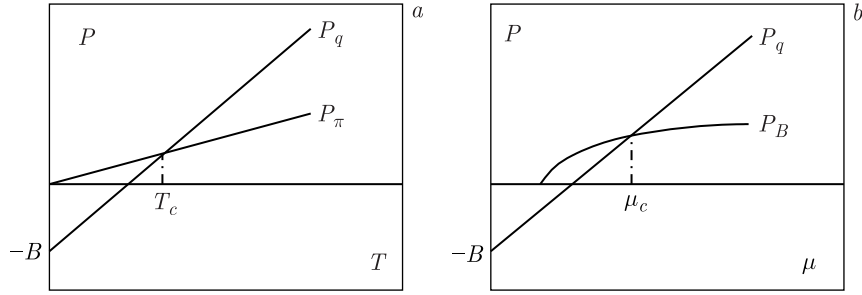


Fig. 4. Pressure comparison at $\mu = 0$ (a) and at $T = 0$ (b)

For $T = 0$, the pressure of extended nucleons is given by

$$P_B(\mu, T = 0) = \frac{P_b(T = 0, \mu)}{1 - n_B(T = 0, \mu)V_e}, \quad (20)$$

where n_B denotes the corresponding density (Eq. (11)) and P_b is the pressure of point-like nucleons of mass M [20],

$$P_b(\mu, T = 0) = \left(\frac{\mu^4}{6\pi^2}\right) \left\{ \left[1 - \left(\frac{M}{\mu}\right)^2\right]^{1/2} \left[1 - \frac{5}{2} \left(\frac{M}{\mu}\right)^2\right] + \frac{3}{2} \left(\frac{M}{\mu}\right)^4 \ln \left[\left(\frac{\mu}{M}\right) \left(1 + \left[1 - \frac{M^2}{\mu^2}\right]^{1/2}\right) \right] \right\}. \quad (21)$$

The corresponding expression for massless quarks is

$$P_q(\mu, T = 0) = \frac{1}{2\pi^2} \left(\frac{\mu}{3}\right)^4 - B, \quad (22)$$

where we have converted the quark baryochemical potential to that of nucleons, $\mu_q = \mu/3$. Again, we equate the two pressures (see Fig. 4, b) to obtain a critical baryochemical potential $\mu_c(B, V_c)$. Here one can as well try to tune bag pressure and hard-core volume to obtain a reasonable threshold.

However, our point in presenting such a toy model hadron–quark pressure comparison is not a quantitative determination of $T_c(B)$ and $\mu_c(B, V_c)$. We only want to illustrate that here in the low baryon density region, the confining bag pressure (as counterpart of the hadron size in percolation) provides the transition and sets the transition scale, whereas at low temperature and high baryon density, this is achieved by two competing effects, the confining bag pressure and the hard-core repulsion.

Obviously, these considerations are a gross oversimplification, since we have neglected the resonance interactions of both pions and nucleons, as well as the role of strange mesons and baryons. We shall include these in the following.

3. THE HADRONIC RESONANCE GAS

For vanishing or low baryon number density, the interactions in a hot hadronic medium are resonance dominated, and hence the system can be described as an ideal gas of all possible resonance species [21, 22], contained in an overall spatial volume V . The grand canonical partition function for such a gas is given by [23, 24]

$$\ln Z(T, \mu, \mu_S, V) = \ln Z_M(T, V, \mu_S) + \ln Z_B(T, \mu, \mu_S, V), \quad (23)$$

where the first term gives the meson and the second, the baryon contributions to the partition function. Baryon number and strangeness are accounted for by the corresponding chemical potentials μ and μ_S , respectively. For the meson contributions, we sum over all possible states i

$$\ln Z_M(T, V, \mu_S) = \sum_{\text{mesons } i} \ln Z_M^i(T, V, \mu_S), \quad (24)$$

with

$$\ln Z_m^i(T, V, \mu_S) = d_i \frac{VT}{2\pi^2} m_i^2 \sum_{n=1}^{\infty} n^{-2} K_2\left(\frac{nm_i}{T}\right) \epsilon^{nS_i\mu_S/T}, \quad (25)$$

where d_i specifies the spin–isospin degeneracy and S_i the strangeness of the state i . For the baryon contributions we have

$$\ln Z_B(T, \mu, \mu_S, V) = \sum_{\text{baryons } i} \ln Z_B^i(T, \mu, \mu_S, V), \quad (26)$$

with

$$\ln Z_B^i(T, \mu, V) = d_i \frac{VT}{2\pi^2} m_i^2 \sum_{n=1}^{\infty} (-1)^{n+1} n^{-2} K_2\left(\frac{nm_i}{T}\right) \epsilon^{n(B_i\mu + S_i\mu_S)/T}, \quad (27)$$

where B_i is the corresponding baryon number of the state i . The above form incorporates Bose–Einstein and Fermi–Dirac statistics; the first term of the sums in Eqs. (25) and (27) is the Boltzmann limit. In all actual calculations we enforce both baryon number and strangeness conservation with a vanishing overall strangeness.

The resonances are confined (colour singlet) $q\bar{q}$ or qqq states of hadronic spatial size. As above, we consider the transition from a confined to a deconfined medium to occur when the hadrons as little bags fuse into one big bag, the quark–gluon plasma [25]; the critical transition density is given by Eq. (8). If we ignore for the moment the contribution of baryons and antibaryons, we can estimate the transition curve in the resonant, low baryon density region by limiting the meson density n_M , obtained from Eq. (25),

$$n_M(T, \mu) = \frac{1.22}{V_h} \simeq 0.57 \text{ fm}^{-3}. \quad (28)$$

This equation can be solved using a resonance gas summation code, summing over all meson states up to mass 2.5 GeV [23]; it leads for $\mu = 0$ to a transition temperature $T_c \simeq 177$ MeV, a value considerably lower than that of pure pion gas case in the previous section.

Just as in the toy model, however, the temperature obtained from Eq. (28) is presumably somewhat too high, since we had required the box to be filled by mesons alone, while in fact baryons and antibaryons can contribute to forming a connecting cluster of hadronic matter. But including the density of baryons and antibaryons in the limiting relation (28) gives at $\mu = 0$ a limiting temperature $T_c \simeq 170$ MeV, only slightly lower, so that the role of the baryons and antibaryons in establishing the boundary is again quite small.

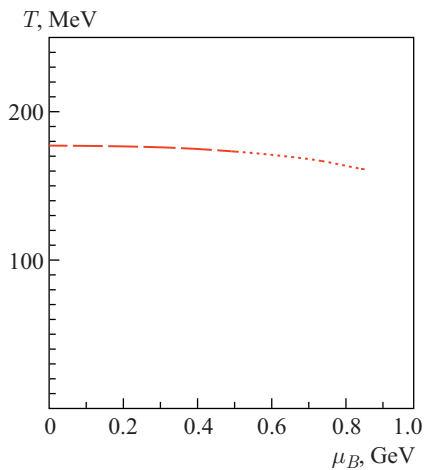


Fig. 5. Transition line in the resonance regime

leading to the fusion into one connected volume [25], and it occurs, as we saw above, already for a pion gas, though at a higher temperature. Thus, the existence of the limit is due to the basic hadronic size [26], the actual value of the transition temperature to the scale specifying the resonance spectrum [22].

If we neglect the interrelation of strangeness and baryon number due to associated production, the mesonic part of the partition function is independent of μ , and hence Eq. (28) leads to a constant T_c for all μ . Taking associated production into account, however, implies with increasing μ an increasing density of strange mesons and thus a (slightly) decreasing temperature. The resulting behavior is shown in Fig. 5.

The deconfinement transition in the resonant region is conceptually a consequence of hadron size and clustering,

An interacting hadron medium can be replaced by an ideal resonance gas only if the interactions are dominantly of resonance nature. As the baryon density increases, however, there are more and more nonresonant contributions, and in the limit of low temperature T and large baryochemical potential μ , i.e., for cold and dense nuclear matter, the nonresonant nuclear forces are the dominant interaction.

We therefore assume as above that in the region of large baryon density, the jamming of baryons with a hard core defines the limit, so that the relevant relation is Eq.(12). To connect this geometric argument with thermodynamics, we again follow the van der Waals approach (11) for baryons and antibaryons, with $V_e = 2V_c$ and $R_c = 0.4$ fm. The resulting hard-core transition curve is shown in Fig.6, together with the bag fusion curve. The $T-\mu$ plane thus shows two distinct regimes: at low μ , hadron percolation through bag fusion, at large μ a first-order mobility or jamming transition.

As already mentioned above, the separate calculation of a bag fusion and a hard-core curve is only an attempt to arrive at a schematic picture as long as we do not have continuum percolation studies for a (μ -determined) mixture of permeable spheres with spheres having a hard core. The curve expected from such a calculation will presumably lead to a transition from one regime to the other at somewhat lower values of μ . In fact, the baryon density becomes equal to the meson density at $\mu \simeq 0.45$ GeV, and therefore this may be close to the point at which the change in the nature of the transition occurs.

4. THE NATURE OF THE TRANSITION

Our considerations up to now specified the limit of hadronic matter, defined as the point of disappearance of the vacuum as a large-scale feature. This point was determined through percolation studies, and the percolation limit is in general not a thermodynamic phase transition. Percolation can thus naturally provide a way to produce a rapid crossover not associated with any singularity of the partition function [27,28]. It should be noted, however, that for spin systems, thermal critical behavior can be formulated in terms of percolation [29–31]. It seems possible to extend this to gauge systems, and first such studies relate the onset of deconfinement at $\mu = 0$ to Polyakov loop percolation [32], analogous to

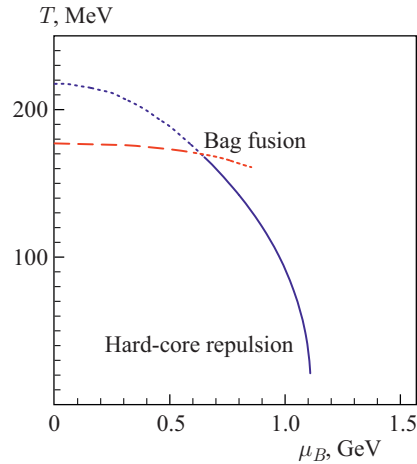


Fig. 6. Bag fusion vs. hard-core transition lines

the onset of magnetization as the percolation of spin clusters. Here it is the onset of large scale disorder, i.e., of the vacuum, which induces critical behavior. From the confined side, we thus have hadronic bag fusion leading to the disappearance of the physical vacuum, while on the deconfined side, formation of disordered clusters in an ordered medium corresponds to the appearance of the vacuum. Based on the spin–gauge universality [33], deconfinement as Polyakov loop percolation could occur as first ($SU(3)$) or second-order ($SU(2)$) phase transition, corresponding to the spontaneous breaking of a global center Z_3 or Z_2 symmetry.

In the case of hard-core percolation, a connection to thermodynamic critical behavior has also been discussed [16]. If a system with hard-core repulsion between its constituents is in addition subjected to a density-dependent negative background potential, first order critical behavior can appear. A classical case is the van der Waals equation. The pressure in our hard-core medium is given by

$$P(T, \mu) = \frac{P_0(T, \mu)}{1 - n(T, \mu)V_e}, \quad (29)$$

where P_0 denotes the pressure of point-like constituents. The density n of the hard-core constituents is given by Eq. (11), and V_e again denotes the random dense packing volume. If we add to this purely repulsive form the density-dependent attractive term

$$P_{\text{vdW}}(T, \mu) = P(T, \mu) - an^2, \quad (30)$$

with constant a , we obtain the van der Waals equation of state with a first-order phase transition ending in a second-order critical point specified by the parameters a and V_e .

5. SUMMARY

We have argued that as function of T and μ , hadronic matter finds itself in two distinct regimes. At low baryon density, the behavior of the system is governed by resonance formation and clustering, with hadronic size and resonance spectrum as relevant parameters. The interaction here is essentially attractive. At high baryon density, in addition to this, there is a repulsive contribution, on the confined side as nuclear repulsion, on the deconfined side as Fermi repulsion between quarks. In our approach, the resulting limit of hadronic matter is in the low baryon density region determined by the percolation of permeable (overlapping) mesons and at high baryon density by the percolation of hard-core baryons. In the latter case, the competition between repulsion and clustering can provide a first-order phase transition. In mesonic percolation there is only clustering; while in general not resulting in thermodynamics critical behavior, it can in specific cases (depending on details of the dynamics) also result in first- or second-order phase transitions.

REFERENCES

1. For a survey, see, e.g., *Karsch F.* Lattice Simulations of the Thermodynamics of Strongly Interacting Elementary Particles and the Exploration of New Phases of Matter in Relativistic Heavy-Ion Collisions // *J. Phys. Conf. Ser.* 2006. V. 46. P. 122.
2. *Fodor Z., Katz S.* Lattice Determination of the Critical Point of QCD at Finite T and μ // *JHEP.* 2002. V. 0203. P. 014.
3. *de Forcrand P., Philipsen O.* The QCD Phase Diagram for Small Densities from Imaginary Chemical Potential // *Nucl. Phys. B.* 2002. V. 642. P. 290.
4. *Lombardo M.-P.* Finite Density QCD via Imaginary Chemical Potential // *Phys. Rev. D.* 2003. V. 67. P. 014505.
5. *Allton C.R. et al.* The Equation of State for Two-Flavor QCD at Nonzero Chemical Potential // *Ibid.* V. 68. P. 014507;
Miau C., Schmidt C. Bulk Thermodynamics and Charge Fluctuations at Nonvanishing Baryon Density // *PoS (LATTICE 2007).* 175.
6. *Stephanov M.A.* Random Matrix Model of QCD at Finite Density and the Nature of the Quenched Limit // *Phys. Rev. Lett.* 1996. V. 76. P. 4472.
7. *Halasz M.A. et al.* On the Phase Diagram of QCD // *Phys. Rev. D.* 1998. V. 58. P. 096007.
8. *Stephanov M.A., Rajagopal K., Shuryak E.* Signatures of the Tricritical Point in QCD // *Phys. Rev. Lett.* 1998. V. 81. P. 4816.
9. *Schwarz T.M., Klevansky S.P., Papp G.* The Phase Diagram and Bulk Thermodynamical Quantities in the NJL Model at Finite Temperature and Density // *Phys. Rev. C.* 1999. V. 60. P. 055205.
10. *Buballa M.* NJL Model Analysis of Quark Matter at Large Density // *Phys. Rep.* 2003. V. 407. P. 205.
11. *Sasaki C., Friman B., Redlich K.* Susceptibilities and the Phase Structure of a Chiral Model with Polyakov Loops // *Phys. Rev. D.* 2007. V. 75. P. 074013.
12. *Meisinger P.N., Ogilvie M.C.* Chiral Symmetry Restoration and $Z(N)$ Symmetry // *Phys. Lett. B.* 1996. V. 379. P. 163;
Fukushima K. Chiral Effective Model with the Polyakov Loop // *Phys. Lett. B.* 2004. V. 591. P. 277;
Ratti C., Thaler M.A., Weise W. Phases of QCD: Lattice Thermodynamics and a Field Theoretical Model // *Phys. Rev. D.* 2006. V. 73. P. 014019.
13. *Castorina P., Redlich K., Satz H.* The Phase Diagram of Hadronic Matter // *Eur. Phys. J. C.* 2009. V. 59. P. 67.
14. See, e.g., *Karsch F., Satz H.* On the Thermodynamics of Extended Hadrons // *Phys. Rev. D.* 1980. V. 21. P. 1168.
15. See, e.g., *Isichenko M.B.* Percolation, Statistical Topography, and Transport in Random Media // *Rev. Mod. Phys.* 1992. V. 64. P. 961.
16. *Kratky K.W.* Is the Percolation Transition of Hard Spheres a Thermodynamic Phase Transition? // *J. Stat. Phys.* 1988. V. 52. P. 1413.
17. *Cleymans J. et al.* On the Phenomenology of Deconfinement and Chiral Symmetry Restoration // *Z. Phys. C.* 1986. V. 33. P. 151.

18. *Rischke D.H. et al.* Excluded Volume Effect for the Nuclear Matter Equation of State // *Z. Phys. C.* 1991. V. 51. P. 488;
Yen G.D. et al. Excluded Volume Hadron Gas Model for Particle Number Ratios in $A + A$ Collisions // *Phys. Rev. C.* 1997. V. 56. P. 2210.
19. *Onoda G.Y., Liniger E.G.* Random Loose Packings of Uniform Spheres and the Dilatancy Onset // *Phys. Rev. Lett.* 1990. V. 22. P. 2727.
20. *Cleymans J., Gavai R.V., Suhonen E.* Quarks and Gluons at High Temperatures and Densities // *Phys. Rep.* 1986. V. 130. P. 217.
21. *Beth E., Uhlenbeck G.E.* The Quantum Theory of the Non-Ideal Gas. II. Behavior at Low Temperatures // *Physica.* 1937. V. 4. P. 915.
22. *Hagedorn R.* Statistical Thermodynamics of Strong Interactions at High Energies // *Nuovo Cim. Suppl.* 1965. V. 3. P. 147; Hadronic Matter near the Boiling Point // *Nuovo Cim. A.* 1968. V. 56. P. 1027.
23. *Braun-Munzinger P., Redlich K., Stachel J.* Particle Production in Heavy-Ion Collisions // *Quark Gluon Plasma 3* / Eds. R. C. Hwa, Xin-Nian Wang, World Sci. Publ., 2003. P. 491.
24. *Karsch F., Redlich K., Tawfik A.* Thermodynamics at Nonzero Baryon Number Density: A Comparison of Lattice and Hadron Resonance Gas Model Calculations // *Phys. Lett. B.* 2003. V. 571. P. 67.
25. *Baacke J.* Thermodynamics of a Gas of MIT Bags // *Acta Phys. Polon. B.* 1977. V. 8. P. 625.
26. *Pomeranchuk I. Ya.* On the Theory of Multiple Particle Production in a Single Collision // *Dokl. AN SSSR.* 1951. V. 78. P. 889.
27. *Satz H.* Deconfinement and Percolation // *Nucl. Phys. A.* 1998. V. 642. P. 130c.
28. *Fortunato S., Satz H.* Cluster Percolation and Pseudocritical Behavior in Spin Models // *Phys. Lett. B.* 2001. V. 509. P. 189.
29. *Fortuin C.M., Kasteleyn P.W.* Phase Transitions in Lattice Systems with Random Local Properties // *J. Phys. Soc. Japan (Suppl.)*. 1969. V. 26. P. 11; On the Random-Cluster Model: I. Introduction and Relation to Other Models // *Physica.* 1972. V. 57. P. 536.
30. *Coniglio A., Klein W.* Clusters and Ising Critical Droplets: A Renormalization Group Approach // *J. Phys. A.* 1980. V. 13. P. 2775.
31. *Blanchard Ph. et al.* On the Kertész Line: Thermodynamic versus Geometric Criticality // *J. Phys. A.* 2008. V. 41. P. 085001.
32. *Fortunato S., Satz H.* Polyakov Loop Percolation and Deconfinement in $SU(2)$ Gauge Theory // *Phys. Lett. B.* 2000. V. 475. P. 311.
33. *Svetitsky B., Yaffe L.G.* Critical Behavior at Finite Temperature Confinement Transitions // *Nucl. Phys. B.* 1982. V. 210. P. 423. [FS6].